C-Peptide Prevents Hyperglycemia-Induced Endothelial Apoptosis Through Inhibition of Reactive Oxygen Species–Mediated Transglutaminase 2 Activation

Mahendra Prasad Bhatt,[1,2] Young-Cheol Lim,[1] JongYun Hwang,[3] SungHun Na,[3] Young-Myeong Kim,[1] and Kwon-Soo Ha[1]

C-peptide is a bioactive peptide with a potentially protective role in diabetes complications; however, its molecular mechanism of protection against cardiovascular damage caused by hyperglycemia-induced apoptosis remains unclear. We investigated the protective mechanism of C-peptide against hyperglycemia-induced apoptosis using human umbilical vein endothelial cells and streptozotocin diabetic mice. High glucose (33 mmol/L) induced apoptotic cell death in endothelial cells via sequential elevation of intracellular Ca^{2+} and reactive oxygen species (ROS) as well as subsequent activation of transglutaminase 2 (TG2). C-peptide (1 nmol/L) prevented endothelial cell death by inhibiting protein kinase C– and NADPH oxidase–dependent intracellular ROS generation and by abolishing high glucose–induced TG2 activation, without affecting intracellular Ca^{2+} levels. Consistently, in the aorta of streptozotocin diabetic mice, hyperglycemia stimulated transamidating activity and endothelial cell apoptosis that was inhibited by C-peptide replacement therapy (35 pmol/min/kg) using osmotic pumps (control and diabetes, $n = 8$; diabetes + C-peptide, $n = 7$). In addition, C-peptide prevented hyperglycemia-induced activation of transamidation activity and apoptosis in the heart and renal cortex of streptozotocin diabetic mice. Thus, C-peptide protects endothelial cells from hyperglycemia-induced apoptotic cell death by inhibiting intracellular ROS-mediated activation of TG2. Furthermore, TG2 may be a promising avenue of therapeutic investigation to treat diabetic vasculopathies. ***Diabetes*** **62:243–253, 2013**

Lack of C-peptide, along with insulin, is the main feature of type 1 diabetes mellitus (DM) and is also observed in progressive β-cell loss in later stage of type 2 DM (1,2). The subsequent hyperglycemia in diabetes is the foremost risk factor for vascular complications due to enhanced rates of cellular apoptosis as observed in retinal pericytes, renal podocytes, and vascular endothelial cells (3,4). Apoptosis in the vasculature has also been associated with pathogenesis and progression of atherosclerosis (5) that causes cardiovascular disease, the leading cause of death worldwide (6).

From the [1]Department of Molecular and Cellular Biochemistry, Kangwon National University School of Medicine, Chuncheon, Kangwon-do, Korea; the [2]Department of Laboratory Medicine, Gandaki Medical College Charak Hospital, Pokhara, Nepal; and the [3]Department of Obstetrics and Gynecology, Kangwon National University School of Medicine, Chuncheon, Kangwon-do, Korea.

Corresponding author: Kwon-Soo Ha, ksha@kangwon.ac.kr.

Received 8 March 2012 and accepted 27 June 2012.

DOI: 10.2337/db12-0293

This article contains Supplementary Data online at http://diabetes.diabetesjournals.org/lookup/suppl/doi:10.2337/db12-0293/-/DC1.

See accompanying commentary, p. 39.

Exposure of endothelial cells to high glucose in diabetes triggers apoptosis, leading to vascular dysfunction (7–10). In hyperglycemia, reactive oxygen species (ROS) generation plays a critical role in mediating endothelial cell apoptosis (11,12). Although activation of NADPH oxidase downstream of protein kinase C (PKC) appears to be a major cytosolic source of ROS generation in diabetic vasculature and kidney (9,11,13), mitochondrial ROS production is also involved in hyperglycemia (14,15). Elevation of intracellular Ca^{2+} is another attribute of apoptotic cell death upon high glucose exposure (16,17). Indeed, intracellular Ca^{2+} and/or ROS can enhance the activation of transglutaminase 2 (TG2), which plays a diverse role in a variety of cellular processes, including cell death, proliferation, differentiation, and migration (18,19). TG2 transamidating activity has been paradoxically reported to either facilitate or attenuate apoptosis in various cell types (20–23). Nevertheless, the role of intracellular TG2 in high glucose–induced endothelial cell apoptosis is not clear.

Human C-peptide is a 31-amino acid peptide that is released into the peripheral circulation in an equimolar concentration with insulin (24). C-peptide is considered a bioactive peptide with diverse tissue- and cell-specific protective roles in various physiologic states and diseases, including diabetic neuropathy, nephropathy, vascular dysfunctions, and inflammation in type 1 DM (2,24–27). C-peptide is potentially beneficial in type 1 DM, as well as in type 2 DM, by preventing smooth muscle cell proliferation, macroangiopathy, and neointima formation (28–30). In addition, C-peptide is believed to exhibit anti-apoptotic effects in diabetic rat hippocampus and in SH-SY5Y cells (31,32). C-peptide was recently reported to decrease NADPH oxidase generation of intracellular ROS in human aortic endothelial cells (33). However, the molecular mechanism(s) underlying the protective role of C-peptide in endothelial cells in diabetes and subsequent vascular complications is still unclear.

In this study, we sought to determine the molecular mechanism by which C-peptide could protect endothelial cells against high glucose–induced apoptosis. We hypothesized that high glucose–induced elevation of intracellular Ca^{2+} and ROS could enhance TG2 activation to mediate endothelial cell apoptosis and that C-peptide might protect endothelial cells from high glucose–induced apoptosis by inhibiting intracellular ROS-mediated activation of TG2. To validate our in vitro findings, we generated streptozotocin diabetic mice and investigated the effects of C-peptide by continuous subcutaneous delivery of human C-peptide as a supplement therapy. We then investigated the role of C-peptide in hyperglycemia-induced activation of transamidating activity and apoptosis in aorta, heart, and renal cortex of diabetic mice.

RESEARCH DESIGN AND METHODS

Cell culture. Human umbilical vein endothelial cells (HUVECs) were isolated from human umbilical cord vein as previously described (34). Cells were maintained at 37°C in a humidified 5% CO_2 incubator in M199 culture media supplemented with 20% FBS, 3 ng/mL basic fibroblastic growth factor, 5 units/mL heparin, 100 IU/mL penicillin, and 100 μg/mL streptomycin. For experiments, cells were incubated overnight in low-serum medium (M199 supplemented as above except 5% FBS and 1 ng/mL basic fibroblastic growth factor) and treated with high glucose (33 mmol/L D-glucose) for the indicated times.

Cell death assay. Cell viability was accessed by 3-(4,5-dimethylthiazol-2-yl)-2,5-diphenyltetrazolium bromide (MTT) reduction assay as described previously (19). Cells were treated with 1 mg/mL MTT solution for 4 h at 37°C, and the insoluble formazan crystals produced by viable cells were dissolved in isopropanol. The absorbance was measured at a wavelength of 570 nm using a microplate reader (Molecular Devices, Sunnyvale, CA). Cell viability is expressed as percentage of control.

The nature of cell death was identified by 3,3′-dihexyloxacarbocyanine iodide ($DiOC_6$)/propidium iodide (PI) double-staining, as described previously (19). Briefly, cells were stained with 50 nmol/L $DiOC_6$ and 10 μg/mL PI for 20 min. Stained cells were analyzed by confocal microscopy (Fluoview-300, Olympus, Japan) and differentiated as viable cells ($DiOC_6^{bright}$/PI negative), early apoptotic cells ($DiOC_6^{dim}$/PI negative), and late apoptotic cells ($DiOC_6^{dim}$/PI positive). Single cell fluorescence intensities were determined using the Fluoview-300 software for the confocal microscope in approximately 700 cells per experiment. Data are displayed as scatter plots with the frequency of early apoptotic cells, late apoptotic cells, and total cell death (sum of early and late apoptotic cells) expressed as percentage of total cells.

Measurement of intracellular ROS generation and Ca^{2+} levels. Intracellular ROS generation was measured as previously described (19). Briefly, cells were treated with 33 mmol/L glucose in the presence of 1 nmol/L C-peptide or heat-inactivated C-peptide in low-serum media (phenol red–free) for the indicated times, followed by incubation with 10 μmol/L 2′,7′-dichlorodihydrofluorescein diacetate in serum- and phenol red–free media for 10 min. Heat-inactivated C-peptide was prepared by boiling at 100°C for 60 min. Coverslips were mounted on a perfusion chamber, and labeled cells were quickly scanned by confocal microscopy. Single cell fluorescence intensities were determined in 30 cells per experiment. The level of intracellular ROS was determined by comparing fluorescence intensities of treated cells with those of control cells (fold).

Intracellular Ca^{2+} levels were monitored as described previously (19). Cells were treated with 33 mmol/L D-glucose for the indicated times in the presence of C-peptide (1 nmol/L) or inhibitors and then incubated with 2 μmol/L Fluo-4 AM for 30 min. Cells were scanned using the confocal microscope. Single cell fluorescence intensities were determined in 30 cells per experiment. Results are expressed as relative fluorescent intensity.

Measurement of in situ transamidating activity in HUVECs. In situ transamidating activity was determined by confocal microscopic assay, as described previously (19). Briefly, cells were incubated for 1 h with 1 mmol/L 5-(biotinamido)pentylamine (BAPA), a pseudosubstrate of TG2, fixed with 3.7% formaldehyde in PBS for 30 min, and permeabilized with 0.2% Triton X-100 in PBS for 30 min. After incubation for 30 min with a blocking solution of 2% BSA in 20 mmol/L Tris (pH 7.6), 138 mmol/L NaCl, and 0.1% Tween 20, cells were incubated with fluorescein isothiocyanate (FITC)-conjugated streptavidin (1:200, v/v) in the blocking solution for 1 h and observed under the confocal microscope. Single cell fluorescence intensities were determined in 30 cells per experiment. Relative TG2 activity was determined by comparing the fluorescence intensities of treated cells with those of control cells (fold).

Transfection of small interfering (si)RNA. HUVECs were transfected with TG2-specific siRNA according to previously described procedures (34). Briefly, cells were transfected with the TG2-siRNA duplex, 5′-AAGAGCGAGAUGAUCUGGAAC-3′, which was synthesized to target the coding sequence of human TG2 mRNA. A noncoding siRNA was used as a control (Dharmacon, Lafayette, CO). Transfection was performed using siLentFect Lipid Reagent (Bio-Rad Laboratories, Hercules, CA) for 24 h.

Western blot analyses. Cells were incubated for 10 min in ice-cold lysis buffer (50 mmol/L HEPES [pH 7.5], 1 mmol/L EDTA, 150 mmol/L NaCl, 1% Triton X-100, 0.1 mmol/L phenylmethylsulfonyl fluoride, 10 μg/mL aprotinin, 10 μg/mL leupeptin), scraped off the culture dish, and whole cell lysates were obtained by centrifugation at 18,000*g* for 10 min at 4°C. Cell lysates were resolved by SDS-PAGE, and transferred to polyvinylidene fluoride membranes. The membranes were blocked with 5% skim milk in Tris-buffered saline with Tween for 1 h, and protein expression was analyzed by probing with antibody against TG2, followed by incubation with a horseradish peroxidase–conjugated secondary antibody.

Generation of diabetic mouse model and C-peptide treatment using osmotic pumps. Six-week-old male C57BL/6 mice were obtained from Nara Biotech (Seoul, Korea). All experiments were performed in accordance with the guidelines of the institutional animal care and use ethics committee of Kangwon National University. Diabetic mice were generated by one intraperitoneal injection of streptozotocin (150 mg/kg body weight) freshly prepared in 100 mmol/L citrate buffer (pH 4.5). Mice were supplied with 10% sucrose overnight to prevent sudden hypoglycemic shock. Sufficient hyperglycemia was observed 2 days after injection, as determined by measuring blood glucose using the Accu-Chek Active blood glucose monitor (Roche Diagnostics GmbH, Germany) and glucosuria using Uriscan (TD Diagnostics, Young-In, Korea). Mice with nonfasting blood glucose levels greater than 16 mmol/L, polyuria, and glucosuria were considered diabetic.

At 1 week after the streptozotocin injection, one group of diabetic mice ($n = 7$) was subcutaneously implanted with Alzet mini-osmotic pump 2004 (DURECT, Cupertino, CA) containing C-peptide in PBS with a delivery rate of 35 pmol/min/kg. The other diabetic ($n = 8$) and control groups ($n = 8$) underwent sham operations. During the continuous subcutaneous C-peptide perfusion, serum C-peptide levels were measured using a C-peptide Enzyme Immunoassay Kit (RayBiotech, Norcross, GA). An additional set of control and diabetic mice ($n = 6$ per group) were prepared for ex vivo experiments.

Tissue collection. Mice were killed by cervical dislocation, and the aorta, heart, and kidneys were dissected. Aortic segments from control ($n = 6$) and diabetic mice ($n = 6$) were collected in culture media for the ex vivo experiment. Aortas for measurement of in vivo transamidating activity and terminal deoxynucleotidyl transferase–mediated dUTP nick-end labeling (TUNEL) assays were immediately fixed with acetone ($n = 8$ for control and diabetes, $n = 7$ for diabetes + C-peptide). Hearts and kidneys were washed, immediately frozen in optimal cutting temperature compound in liquid nitrogen, and stored at −80°C before immunohistologic studies.

Measurement of transamidating activity in tissues. To investigate the effect of ex vivo C-peptide treatment on transamidating activity of diabetic mice aorta, aortic segments from each diabetic mouse ($n = 6$) were cut and divided into three groups: the first group was used for ex vivo treatment of C-peptide, second for cystamine, and third for vehicle treatment against control group ($n = 6$). Aortic segments were incubated for 1 h at 37°C with 1 mmol/L BAPA and 5 nmol/L C-peptide or 50 μmol/L cystamine in serum-free M199 media, fixed for 10 min with cold acetone, and incubated for 1 h with FITC-conjugated streptavidin (1:200, v/v). Tissues were double-stained overnight with goat-polyclonal platelet endothelial cell adhesion molecule-I antibody, followed by probing with Alexa-546-conjugated rabbit anti-goat IgG. Aortic segments were cut to open longitudinally, mounted en face on glass slides, and observed under the confocal microscope.

To study the effect of in vivo C-peptide treatment on transamidating activity of diabetic mice, aorta or 7-μm hearts or kidneys cryosections were immediately fixed with cold acetone for 10 min and incubated with 1 mmol/L BAPA for 1 h. Tissue samples were then permeabilized with 0.2% Triton X-100 in PBS for 30 min, blocked with 1% BSA in 0.1 mol/L Tris-HCl, and incubated with FITC-conjugated streptavidin (1:200, v/v). Aortic tissues were double-stained with goat-polyclonal platelet endothelial cell adhesion molecule-I antibody and observed under the confocal microscope as described for ex vivo experiments.

TUNEL assay. Aortic segments or frozen tissue sections were fixed for 15 min with 1% (w/v) paraformaldehyde in PBS, followed by treatment for 30 min with 70% (v/v) ethanol on ice. TUNEL staining was performed using reagents from the APO-BrdU TUNEL Assay Kit (Molecular Probes; Eugene, OR). Briefly, fixed tissues were incubated for 1 h at 37°C with a DNA-labeling solution containing terminal deoxynucleotidyl transferase and 5-bromo-2-deoxyuridine in reaction buffer. Tissues were incubated for 30 min with Alexa Fluor 488 dye-labeled 5-bromo-2-deoxyuridine antibody and costained with 1 μmol/L Hoechst dye 33342 for 15 min. Mounted tissue samples were observed under the confocal microscope.

Statistics. Data processing was performed using Origin 6.1 software (OriginLab, Northampton, MA). Statistical significance was determined using ANOVA. A value of $P < 0.05$ was considered statistically significant.

RESULTS

C-peptide inhibits high glucose–induced apoptosis. High glucose decreased the viability of HUVECs dramatically, and this effect was overcome by 1 nmol/L C-peptide (Fig. 1*A*). The high glucose–induced decrease in cell

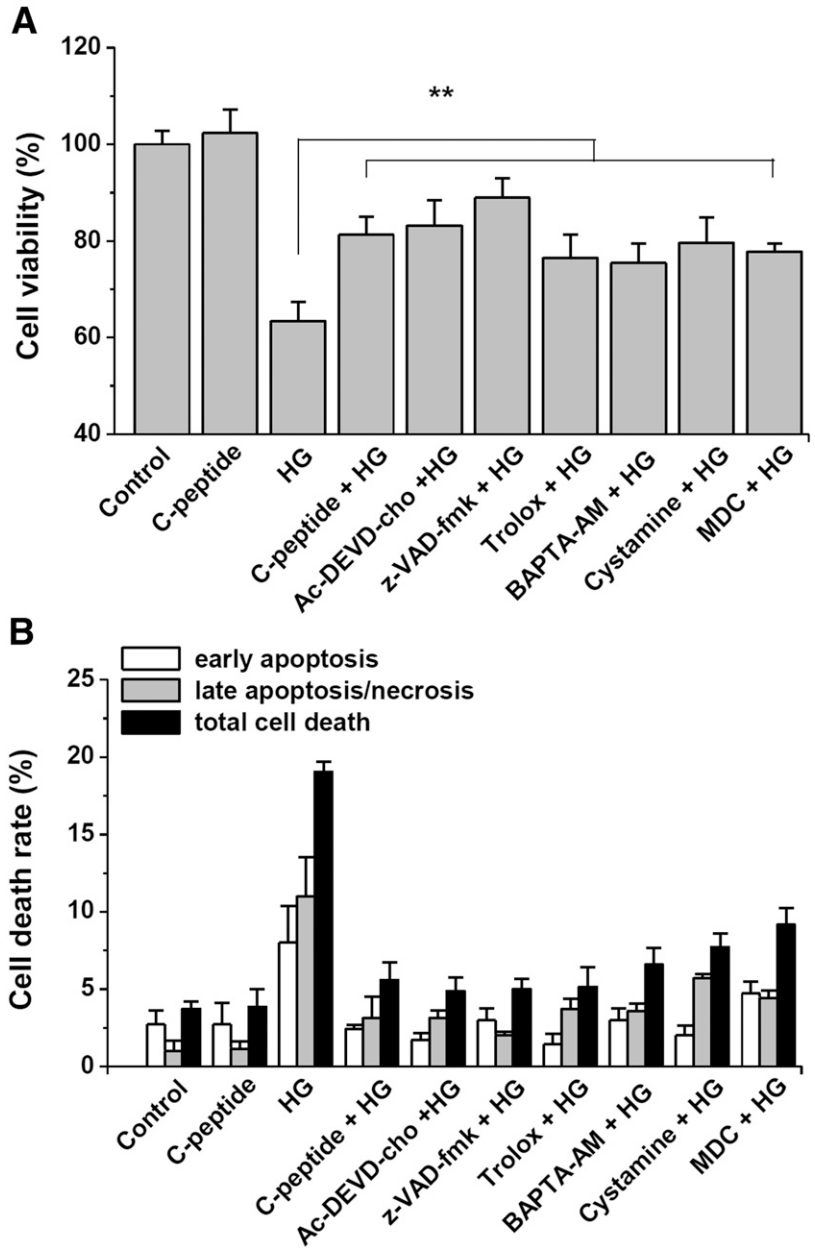

FIG. 1. C-peptide and inhibitors of intracellular ROS, Ca^{2+}, and TG2 inhibit high glucose (HG)–induced apoptotic cell death in HUVECs. Confluent cells were preincubated with 1 nmol/L C-peptide, 5 μmol/L Ac-DEVD-cho, 1 μmol/L Z-VAD-fmk, 0.5 mmol/L Trolox, 5 μmol/L BAPTA-AM, 50 μmol/L cystamine, or 10 μmol/L monodansylcadaverine (MDC) for 30 min, followed by incubation with HG (33 mmol/L D-glucose) for 72 h. *A*: Cell viability was determined using an MTT reduction assay. *B*: HG-induced apoptotic cell death was measured by $DiOC_6$/PI double-staining. Early and late apoptotic cell death rates were determined as described in RESEARCH DESIGN AND METHODS. Results are expressed as mean ± SD from three independent experiments. **$P < 0.01$.

viability was also inhibited by a caspase-3 inhibitor, Ac-DEVD-cho, and a broad-spectrum caspase inhibitor, Z-VAD-fmk ($P < 0.01$). Glucose treatment increased the number of early and late apoptotic cells, as evaluated by DiOC6/PI staining, and cell death was prevented by C-peptide, Ac-DEVD-cho, or Z-VAD-fmk (Fig. 1*B*).

Roles of intracellular ROS and Ca^{2+} and TG2 in high glucose–induced cell death. Because TG2 is activated by increased intracellular ROS and/or Ca^{2+} (18,19,35), we examined the role of intracellular ROS and Ca^{2+} and TG2 in high glucose–induced apoptosis in HUVECs. Trolox, a ROS scavenger, and 2–*Bis* (2-aminophenoxy) ethane-*N*,*N*,*N*′,*N*′-tetraacetic acid tetrakis (acetoxymethyl ester) (BAPTA-AM), a Ca^{2+} chelator, significantly prevented the decrease in cell viability induced by high glucose ($P < 0.01$; Fig. 1*A*). Consistently, these inhibitors also prevented high glucose–induced apoptosis, as assessed by $DiOC_6$/PI double-staining (Fig. 1*B*).

High glucose–induced cell death was significantly reversed by the transglutaminase inhibitors cystamine and monodansylcadaverine ($P < 0.01$; Fig. 1*A*). A similar inhibitory effect on apoptosis was observed with $DiOC_6$/PI double-staining (Fig. 1*B*). TG2 siRNA suppressed TG2 expression in a dose-dependent manner (Fig. 2*A*). TG2 siRNA inhibited high glucose–induced cell death in a dose-dependent manner as estimated by MTT assay, with

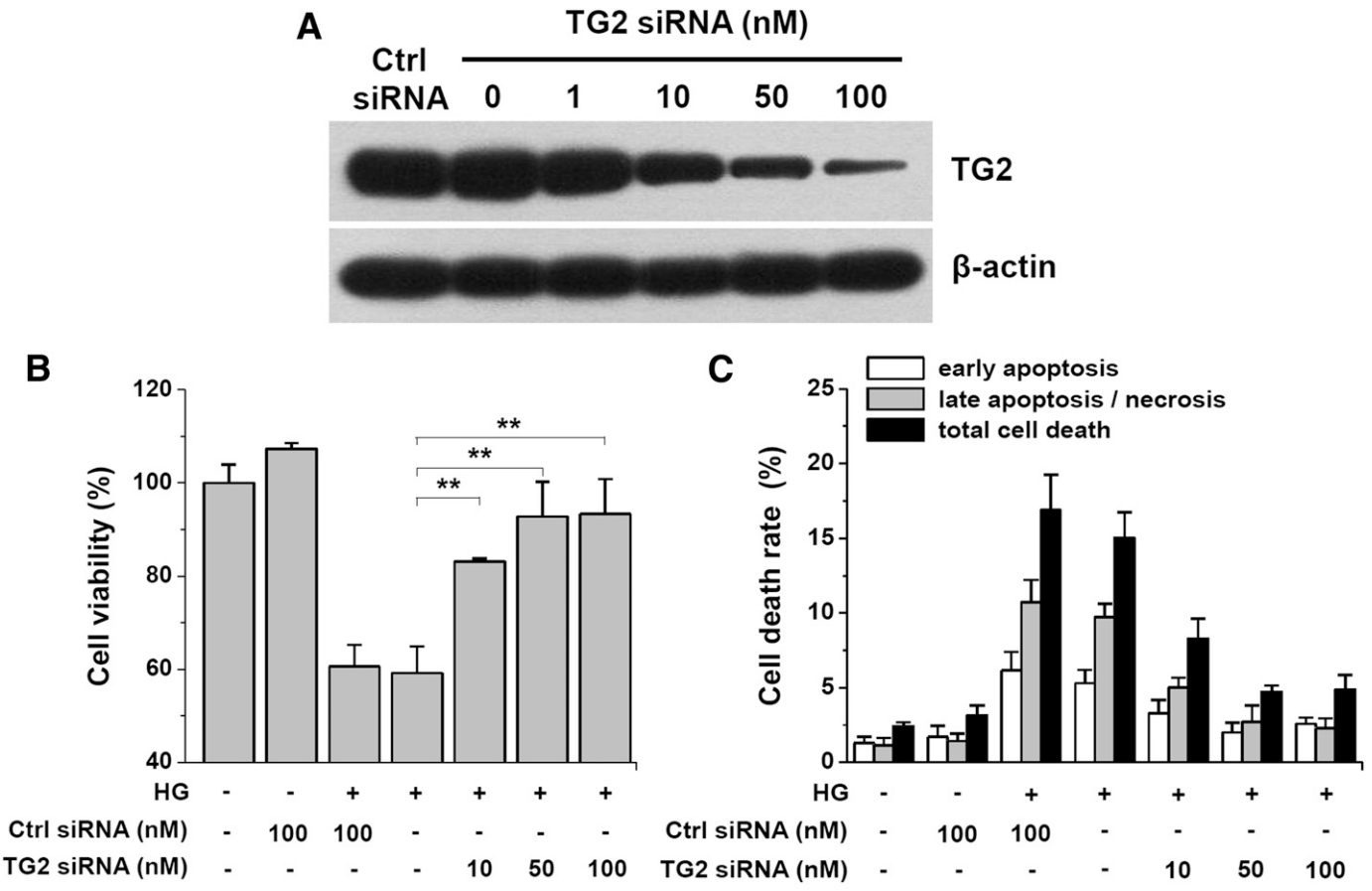

FIG. 2. TG2 siRNA prevents high glucose (HG)–induced apoptotic cell death. Cells were transfected with the indicated concentrations of human TG2–specific siRNA (TG2 siRNA) or control (Ctrl) siRNA and incubated with HG (33 mmol/L D-glucose) for 72 h. *A*: TG2 siRNA inhibits TG2 expression in a concentration-dependent manner. Dose-dependent recovery of cell viability (*B*) and decrease in cell death rate (*C*) by TG2 siRNA. Results are expressed as mean ± SD from three independent experiments. **$P < 0.01$.

significant effect at 10 nmol/L ($P < 0.01$; Fig. 2*B*). TG2 siRNA also prevented the apoptosis observed with $DiOC_6$/PI double-staining (Fig. 2*C*).

Prevention of high glucose–induced generation of intracellular ROS. High D-glucose increased intracellular ROS in a time-dependent manner, with significant stimulation at 48 h ($P < 0.001$), whereas L-glucose did not (Fig. 3*A*). As expected, Trolox inhibited ROS generation in a dose-dependent manner (Fig. 3*B*). In addition, BAPTA-AM inhibited ROS generation in a dose-dependent manner (Fig. 3*B*), indicating the importance of intracellular Ca^{2+} in high glucose–induced ROS generation.

Consistent with previous reports (9,11), the selective PKC inhibitors GF109203x and Ro-31-8220 blocked ROS generation in a dose-dependent manner (Fig. 3*C*). ROS generation was also prevented by apocynin and diphenylene iodonium (Fig. 3*D*), inhibitors of NADPH oxidase (36). These results demonstrate that high glucose–induced ROS is generated by the pathway(s) involving PKC and NADPH oxidase (Fig. 3*C* and *D*). We then examined whether mitochondria participate in ROS generation, as reported previously (14,15). Rotenone, a complex I inhibitor of the mitochondrial electron transport chain, did not inhibit ROS production (Fig. 3*E*). Carbonyl cyanide *m*-chlorophenyl hydrazone and dinitrophenol, uncouplers of oxidative phosphorylation that abolish the mitochondria proton gradient, partially inhibited the ROS generation in response to high glucose (Fig. 3*E*) compared with apocynin and diphenylene iodonium.

C-peptide prevented high glucose–induced ROS generation in a dose-dependent manner, with maximal inhibition with 1 nmol/L (Fig. 4*A*). However, heat-inactivated C-peptide (1 nmol/L) had no inhibitory effect (Fig. 4*B*). Thus, it is likely that C-peptide prevents apoptosis in endothelial cells via inhibiting ROS generation.

Intracellular Ca^{2+} acts upstream of intracellular ROS and is unaffected by C-peptide. High D-glucose increased intracellular Ca^{2+} in a time-dependent manner, with a significant increase at 24 h ($P < 0.001$; Fig. 4*C*). L-Glucose treatment had no effect on the Ca^{2+} level. As expected, the high glucose–induced elevation in intracellular Ca^{2+} was inhibited by BAPTA-AM in a dose-dependent manner (Fig. 4*D*). However, Trolox had no effect on Ca^{2+} elevation (Fig. 4*D*), indicating that intracellular ROS are not involved in the glucose-induced elevation in intracellular Ca^{2+}. Furthermore, C-peptide did not affect the Ca^{2+} increase at any concentration tested (Fig. 4*E*).

C-peptide regulates TG2 activity by inhibiting high glucose–induced ROS generation. High D-glucose increased transamidating activity in a time-dependent manner, with significant stimulation at 24 h ($P < 0.05$), whereas L-glucose had no effect (Fig. 5*A*). However, high glucose had no effect on the expression of TG2 (data not shown). Transfection with TG2 siRNA inhibited high glucose–induced stimulation of transamidating activity in a dose-dependent manner, with significant effect at 10 nmol/L (Fig. 5*B*). As

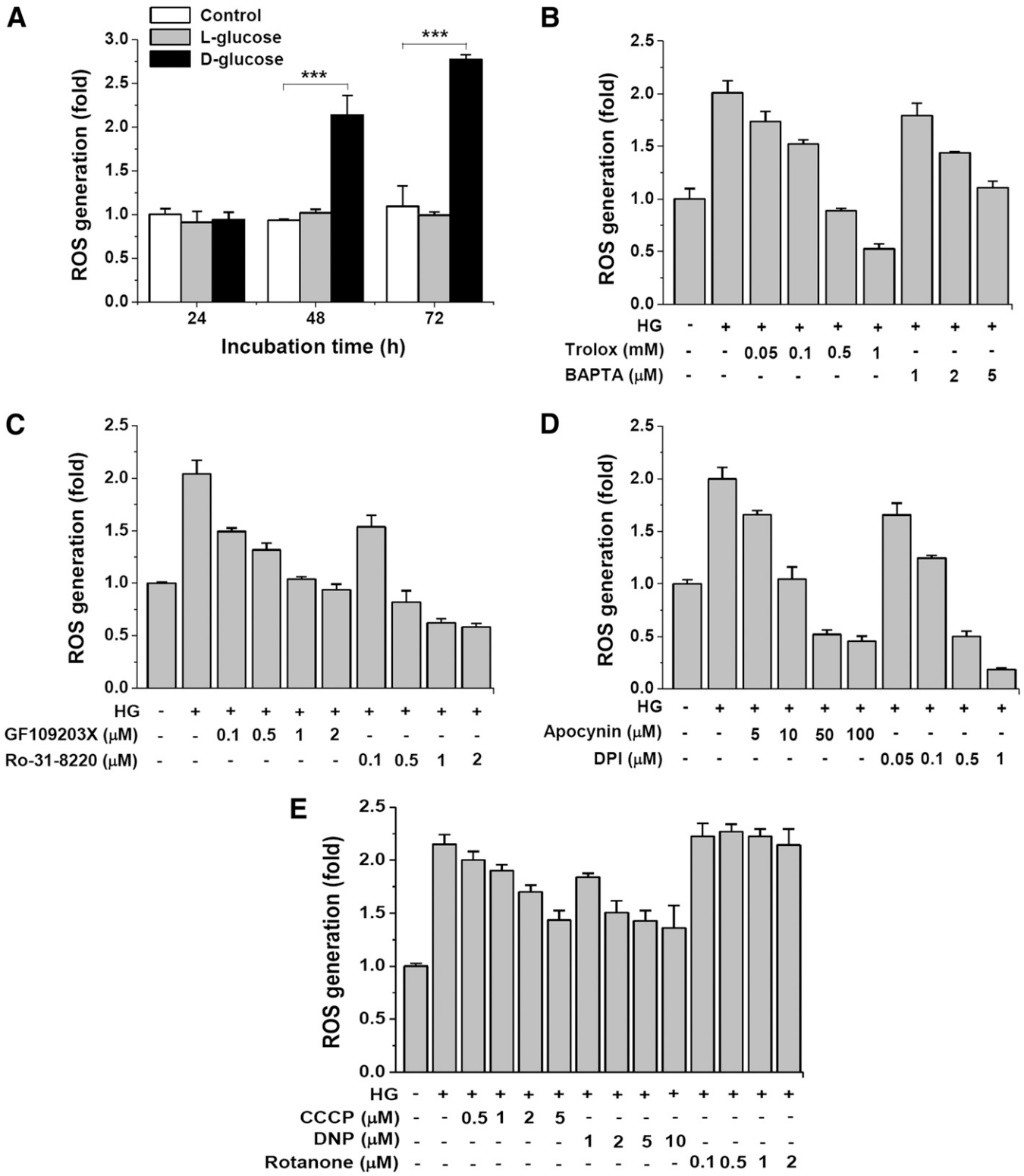

FIG. 3. High glucose (HG)–induced generation of intracellular ROS is prevented by various inhibitors. Cells were incubated with HG (33 mmol/L D-glucose) in the presence of the indicated inhibitors for 48 h, and the levels of intracellular ROS were determined as described in RESEARCH DESIGN AND METHODS. *A*: Time course changes in intracellular ROS by control, L-glucose, and D-glucose. Dose-dependent inhibition of HG-induced ROS generation by Trolox and BAPTA-AM (*B*), PKC inhibitors (*C*), NADPH oxidase inhibitors DPI (diphenylene iodonium) and apocynin (*D*), and carbonyl cyanide *m*-chlorophenyl hydrazone (CCCP), dinitrophenol (DNP), and rotenone (*E*). Results are expressed as mean ± SD from three independent experiments. ***$P < 0.001$.

expected, cystamine and monodansylcadaverine inhibited the high glucose–induced increase in transamidating activity in dose-dependent manners (Fig. 5*C*). The increased transamidating activity was also inhibited by Trolox and BAPTA-AM (Fig. 5*D*), indicating that high glucose stimulated TG2 by elevating intracellular ROS and Ca^{2+} levels. C-peptide prevented the high glucose–induced transamidating activity in a dose-dependent manner, with

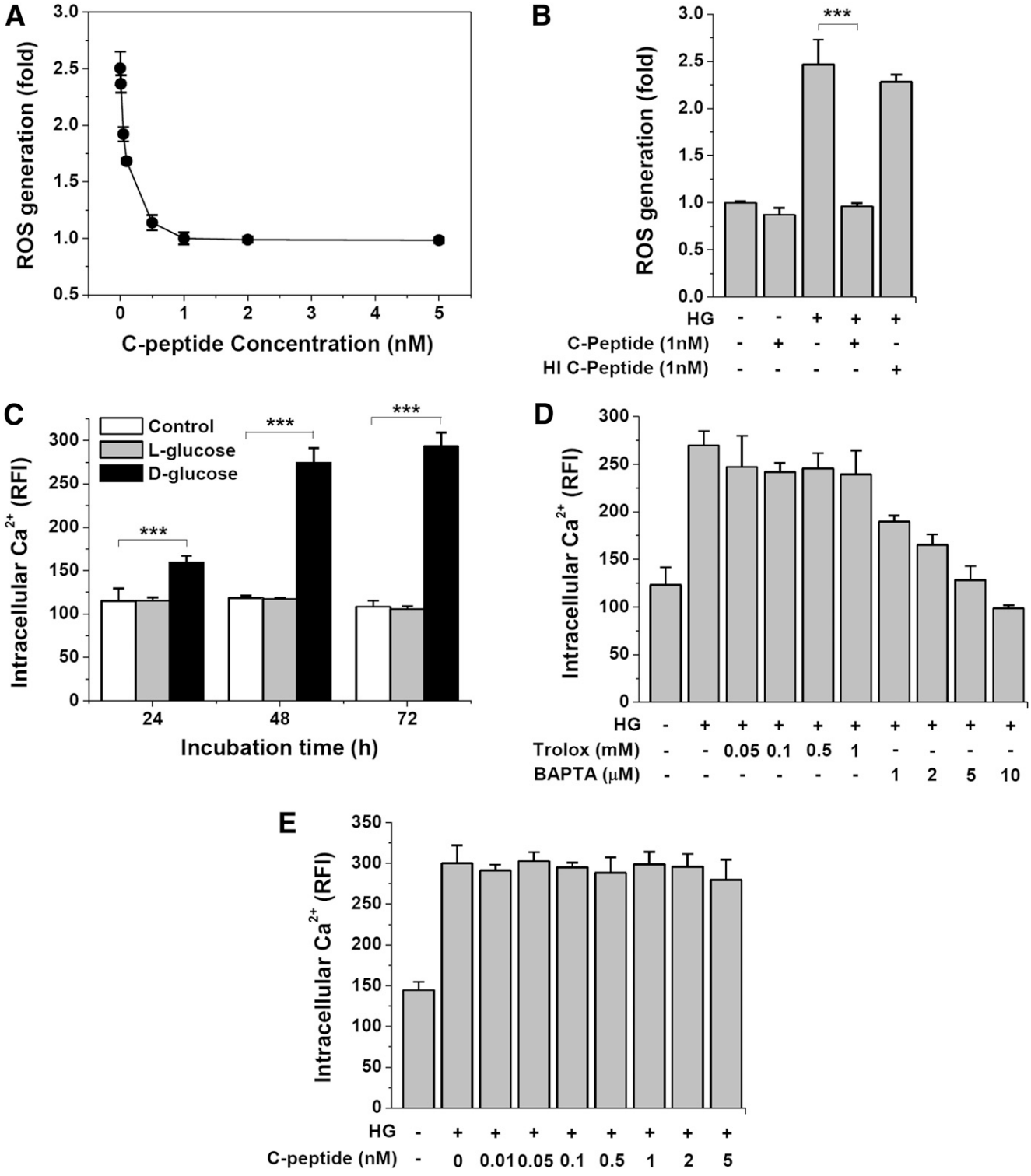

FIG. 4. C-peptide inhibits high glucose (HG)–induced ROS generation but has no effect on intracellular Ca^{2+}. Cells were incubated with HG (33 mmol/L D-glucose) in the presence of the indicated concentrations of C-peptide, Trolox, and BAPTA-AM for 48 h, and intracellular ROS and Ca^{2+} levels were determined as described in RESEARCH DESIGN AND METHODS. *A*: Dose-dependent inhibition of HG-induced ROS generation by C-peptide. *B*: Heat-inactivated (H1) C-peptide (1 nmol/L) has no effect on HG-induced ROS generation. *C*: Time course changes in intracellular Ca^{2+} level by control, L-glucose, and D-glucose. *D*: BAPTA-AM, but not Trolox, has a dose-dependent inhibitory effect on HG-induced elevation in intracellular Ca^{2+} levels. *E*: C-peptide does not inhibit HG-induced elevation of intracellular Ca^{2+}. Results are expressed as mean ± SD from three independent experiments. ***$P < 0.001$.

a maximal inhibition at 1 nmol/L (Fig. 5*E*). These data suggest that C-peptide protects endothelial cells from high glucose–induced apoptosis by inhibiting intracellular ROS-mediated activation of TG2.

Ex vivo treatment of C-peptide in aortic segments of streptozotocin diabetic mice inhibits hyperglycemia-stimulated transamidating activity. Transamidating activity was activated in aortic segments of diabetic mice

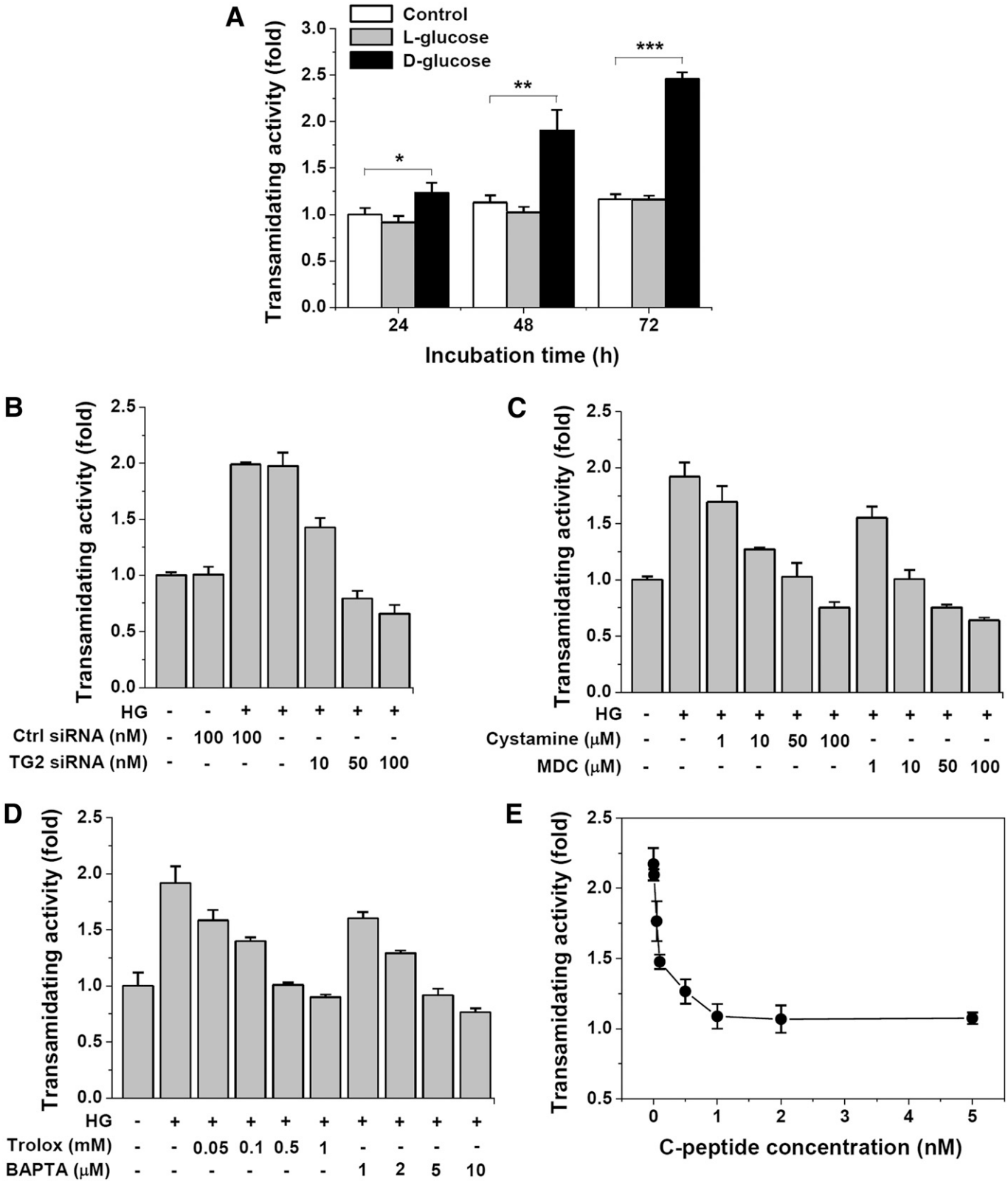

FIG. 5. High glucose (HG)-induced activation of TG2 is inhibited by various inhibitors or C-peptide. Cells were incubated with HG (33 mmol/L D-glucose) for 48 h in the presence of the indicated concentrations of TG2 siRNA or control (Ctrl) siRNA (*B*), inhibitors (*C* and *D*), or C-peptide (*E*). *A*: Time course of TG2 transamidating activity in control, L-glucose, and D-glucose. Dose-dependent inhibition of HG-induced transamidating activity by TG2 siRNA (*B*), cystamine and monodansylcadaverine (MDC) (*C*), Trolox and BAPTA-AM (*D*), or C-peptide (*E*). Results are expressed as mean ± SD from three independent experiments. *$P < 0.05$, **$P < 0.01$, ***$P < 0.001$.

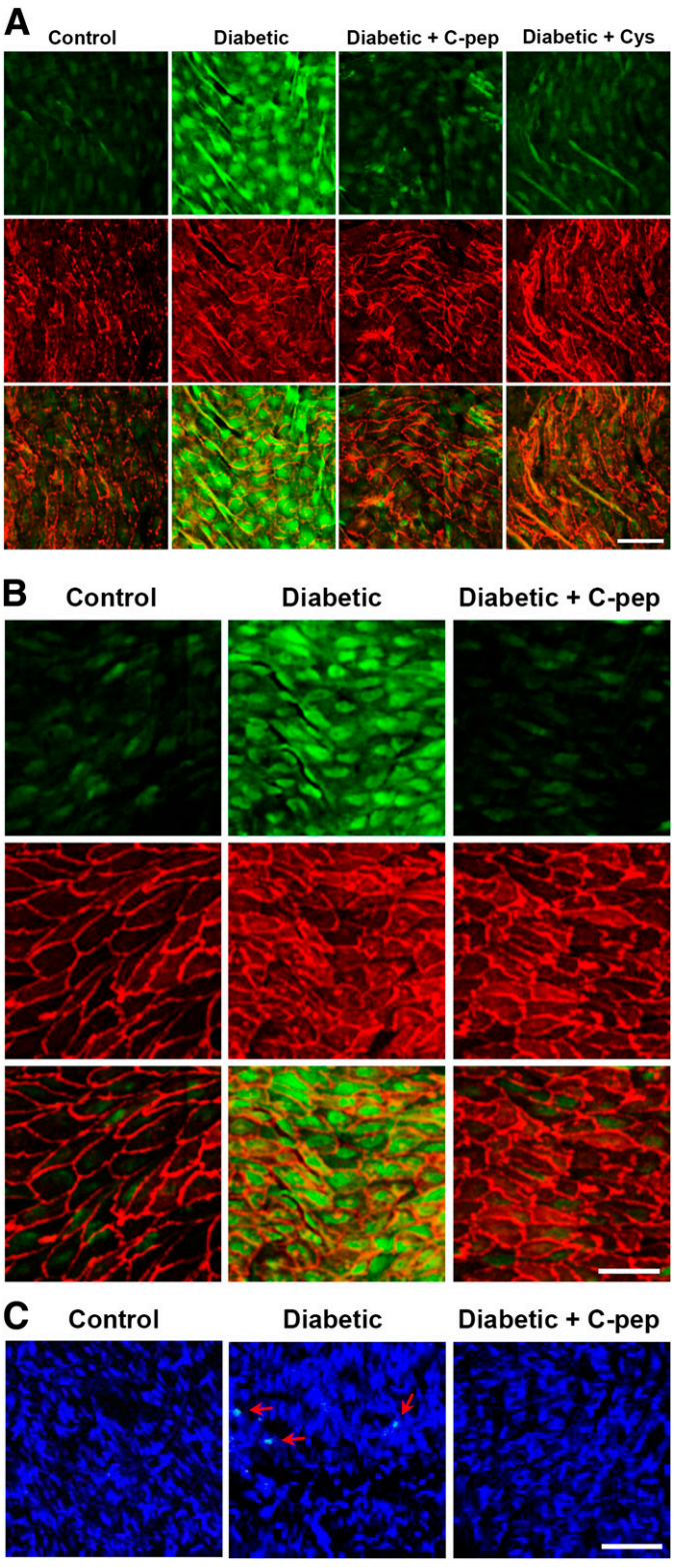

FIG. 6. C-peptide inhibits hyperglycemia-induced stimulation of transamidating activity and apoptosis in mice aortic segments. Transamidating activity (green) in aortic segments was double-stained with endothelial cell marker platelet endothelial cell adhesion molecule-I (red). *A*: Inhibition of hyperglycemia-induced stimulation of transamidating activity by ex vivo treatment of C-peptide (C-pep) or cystamine (Cys; n = 6 per group). *B* and *C*: C-peptide replacement therapy inhibits hyperglycemia-induced stimulation of transamidating activity and apoptosis in vivo (n = 8 for control and diabetes, n = 7 for diabetes + C-peptide). *C*: Apoptotic cells in aortic segments were stained by TUNEL (green, indicated by arrows) with nuclear counterstaining using Hoechst dye 33258 (blue). Bar: 50 μm. (A high-quality color representation of this figure is available in the online issue.)

(Fig. 6*A*). Transamidating activity was observed in cells stained with platelet endothelial cell adhesion molecule, indicating transamidating activity in aortic endothelial cells. However, incubating the segments with 5 nmol/L C-peptide inhibited hyperglycemia-induced activation of transamidating activity. In addition, cystamine inhibited the transamidating activity stimulated by hyperglycemia. Thus, hyperglycemia elevates transamidating activity, and ex vivo treatment of C-peptide inhibits transamidating activity stimulated by hyperglycemia in aorta of diabetic mice.

C-peptide replacement therapy inhibits hyperglycemia-induced activation of transamidating activity and prevents apoptosis in aortic endothelium of streptozotocin diabetic mice. Five-week diabetic mice (n = 8) showed loss of body weight, increased rate of food and water consumption, and severe hyperglycemia (30.15 mmol/L) with glucosuria, compared with nondiabetic controls (n = 8; Supplementary Table 1). However, these parameters were not improved in diabetic mice supplemented with C-peptide (28.73 mmol/L; n = 7). Serum C-peptide levels significantly decreased in untreated diabetic mice ($P < 0.001$) and were fully restored to the normal physiologic range (2.40 nmol/L) in diabetic mice supplemented with C-peptide using osmotic pumps (Supplementary Table 1).

Consistent with our results from ex vivo experiments, transamidating activity was significantly elevated in diabetic mice, and C-peptide supplement prevented hyperglycemia-induced stimulation of transamidating activity (Fig. 6*B*). Apoptotic cells in aortic segments of diabetic mice were investigated by double-staining with TUNEL (green) and Hoechst 33342 dye (blue). A significant number of TUNEL-positive cells were observed in the endothelial layer of diabetic mice aortic segments. However, apoptotic cells were rarely observed in aortic segments of nondiabetic control and C-peptide supplemented mice (Fig. 6*C*). Thus, hyperglycemia stimulated transamidating activity and apoptosis in diabetic mice, and this was prevented by the addition of C-peptide.

C-peptide prevents hyperglycemia-induced activation of transamidating activity and apoptosis in heart and renal cortex of streptozotocin diabetic mice. Increased transamidating activity was observed in the myocardium and myocardial blood vessels (indicated by arrow) of diabetic mice compared with nondiabetic controls (Fig. 7*A*). However, C-peptide inhibited the activation of transamidating activity by hyperglycemia. TUNEL staining showed apoptotic cells in heart sections of diabetic mice, whereas apoptotic cells were rarely observed in heart tissue of nondiabetic control and C-peptide–supplemented diabetic mice (Fig. 7*B*). In addition, C-peptide prevented hyperglycemia-induced activation of transamidating activity and apoptosis in the renal cortex of diabetic mice (Fig. 7*C* and *D*). Our data suggest that C-peptide protects against hyperglycemia-induced apoptosis, probably by inhibiting TG2 transamidating activity in the aorta, heart, and kidney tissues of diabetic mice.

DISCUSSION

C-peptide is considered a bioactive peptide for amelioration of diabetes-induced complications, including

neuropathy, nephropathy, and vascular dysfunction (2,24). In this study, we explored the preventive role of C-peptide against apoptosis induced by hyperglycemia in HUVECs and the endothelium of diabetic mice aorta. C-peptide replacement therapy has been investigated in diabetic neuropathy and nephropathy (24–26), but not in diabetic cardiovascular complications caused by hyperglycemia-induced apoptosis. Therefore, we used replacement therapy to investigate the protective role of C-peptide against high glucose–induced apoptosis in endothelial cells as well as hyperglycemia-induced damage to the aorta and heart, in parallel with renal cortex.

Growing evidence has demonstrated that ROS generation and Ca^{2+} overload are involved in a variety of cell death mechanisms, including high glucose–induced apoptosis (11,12,16,17). We investigated sequentially activated biochemical events, including elevation of intracellular Ca^{2+} and ROS and activation of TG2, in high glucose–induced apoptosis of HUVECs. C-peptide treatment and inhibition of intracellular Ca^{2+} and ROS, as well as TG2 activation, adequately prevented high glucose–induced apoptosis of endothelial cells. We demonstrated caspase-dependent apoptosis of endothelial cells in response to high glucose by $DiOC_6$/PI double-staining and cell death prevention with a caspase-3 inhibitor, Ac-DEVD-cho, and a broad-spectrum caspase inhibitor, Z-VAD-fmk. Thus, we found the molecular events involving intracellular ROS and TG2 are regulated by a C-peptide–signaling pathway that prevents high glucose–induced apoptosis of HUVECs.

High glucose activated TG2 through sequential elevation of intracellular Ca^{2+} and ROS levels in HUVECs (Fig. 8). High glucose–induced generation of intracellular ROS was blocked using BAPTA-AM and selective PKC inhibitors, indicating that ROS generation was triggered by elevated intracellular Ca^{2+} and/or Ca^{2+}-dependent PKC activation, consistent with previous reports (36). Intracellular ROS generation by high glucose was completely inhibited by NADPH oxidase inhibitors and partially prevented by uncouplers of mitochondrial oxidative phosphorylation. These results suggest that intracellular ROS are mainly generated by a mechanism involving Ca^{2+}-activated PKC and NADPH oxidase, with less contribution from the mitochondria. Further, intracellular ROS were not involved in the elevation of intracellular Ca^{2+}. Consistent with a previous report (19), TG2 activation by high glucose was prevented by Trolox and BAPTA-AM. Thus, it seems likely that high glucose–induced intracellular Ca^{2+} stimulates intracellular ROS generation via Ca^{2+}-activated PKC and NADPH oxidase that results in TG2 activation in endothelial cells.

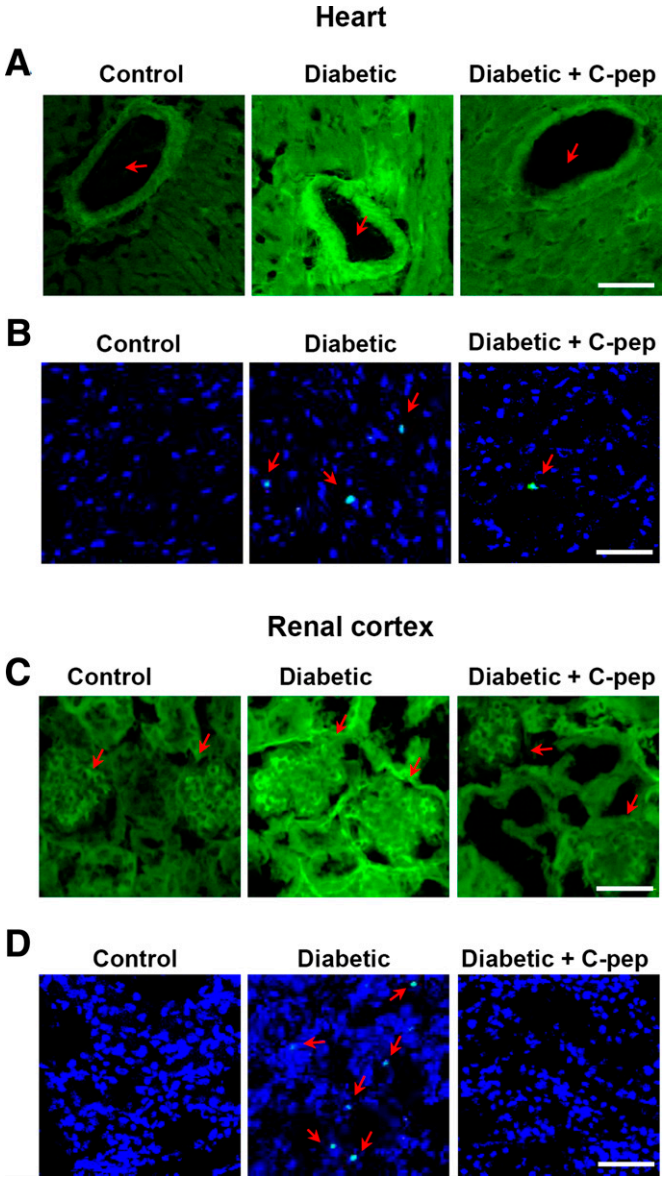

FIG. 7. C-peptide inhibits hyperglycemia-induced stimulation of transamidating activity and apoptosis in heart and renal cortex. In vivo treatment of C-peptide (C-pep) using osmotic pumps inhibits transamidating activity and apoptosis stimulated by hyperglycemia in heart (*A* and *B*) and renal cortex (n = 8 for control and diabetes, n = 7 for diabetes + C-peptide) (*C* and *D*). Transamidating activity was determined by confocal microscopy (green) in heart (*A*) and renal cortex tissues (*C*). Arrows indicate myocardium and associated blood vessels (*A*) and renal cortex, including glomeruli (*C*). Apoptotic cells were stained with TUNEL (green, indicated by arrows) in heart (*B*) and renal cortex tissues (*D*). Nuclei were visualized with Hoechst dye 33258 (blue). Bar: 50 μm. (A high-quality color representation of this figure is available in the online issue.)

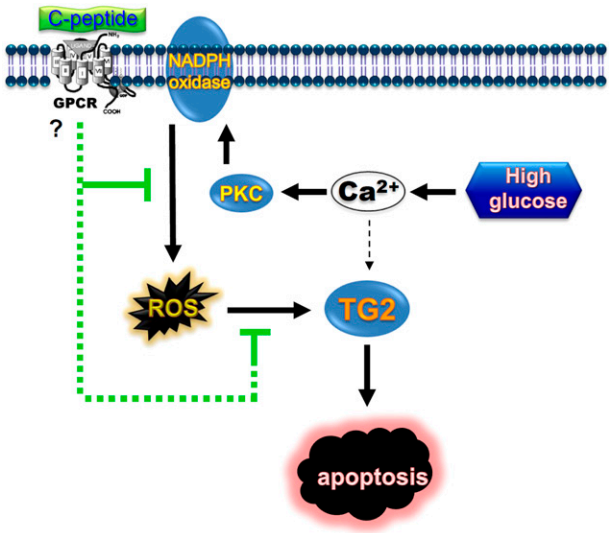

FIG. 8. Proposed mechanism for C-peptide prevention of hyperglycemia-induced endothelial apoptosis via inhibition of ROS-mediated TG2 activation. GPCR, guanosine triphosphate-binding protein-coupled receptor. (A high-quality color representation of this figure is available in the online issue.)

To our knowledge, this is the first study to report that C-peptide (1 nmol/L) ameliorates hyperglycemia-induced apoptosis in endothelial cells via inhibiting intracellular ROS-mediated activation of intracellular TG2 (Fig. 8). Consistently, hyperglycemia stimulated transamidating activity in endothelial cells of diabetic mice aortic segments that was prevented by ex vivo treatment with C-peptide (5 nmol/L) and cystamine. Further, hyperglycemia-induced stimulation of in vivo transamidating activity in diabetic mice was normalized by C-peptide supplement therapy that maintained the physiologic serum level (2.4 nmol/L; Supplementary Table 1) in aortic endothelial cells, cardiac tissues, and renal cortex. Apoptotic cells were observed in aortic endothelium, heart, and renal cortex of diabetic mice but were rarely detected in C-peptide–supplemented diabetic mice. Thus, these in vivo observations support our in vitro findings and provide strong evidence for the antiapoptotic effect of C-peptide through inhibition of hyperglycemia-induced transamidating activity in diabetic mice.

Interestingly, C-peptide prevented high glucose–induced apoptosis by inhibiting TG2 activation through intracellular ROS rather than Ca^{2+}, but high glucose activated TG2 through sequential elevation in intracellular Ca^{2+} and ROS in endothelial cells. Although Ca^{2+} is a cofactor for transamidating activity of TG2 (18), C-peptide inhibited TG2 transamidating activity with no inhibitory effect on intracellular Ca^{2+} elevation by high glucose. In addition, Trolox prevented activation of transamidating activity and apoptotic cell death in response to high glucose but had no effect on intracellular Ca^{2+}, indicating elevated intracellular Ca^{2+} is not enough for high glucose–induced apoptosis in endothelial cells. Thus, elevated intracellular Ca^{2+} and subsequent ROS generation are postulated to be vital indices for high glucose–induced TG2 activation; however, an increase in Ca^{2+} alone may be necessary but not sufficient for TG2-dependent endothelial cell apoptosis without ROS generation.

Similar beneficial effects of C-peptide were also reported by Sima and colleagues (31,32) against high glucose–induced apoptosis of SH-SY5Y cells and hippocampal apoptosis of type 1 DM rats. However, action mechanism(s) of C-peptide for the bioactive roles may remain equivocal until elucidation of its specific receptor signaling. It was initially suggested that C-peptide binds to specific G protein-coupled receptors, providing a molecular basis for its biologic effects (37), whereas other hypotheses proposed that cellular internalization of C-peptide might achieve its molecular effects (38). However, its specific receptor-mediated signaling is still ambiguous. C-peptide exhibits beneficial effects in cells as well as in diabetic animal models with a broad range of cellular signaling, including activation of Akt, extracellular signal–related kinase 1/2, endothelial nitric oxide synthase, and Na^+/K^+-ATPase (2,24). In addition, C-peptide also shows insulinomimetic effect through inhibition of protein tyrosine phosphatase activity and autophosphorylation and activation of insulin receptor substrate-1, without direct binding to insulin receptor (39,40). Therefore, receptor identification is warranted to discover the specific signaling pathways and to explain the mechanisms and role of C-peptide in diabetes complications. Although C-peptide is considered beneficial in type 1 DM, it should not be disregarded in late-stage and obesity-associated type 2 DM, in which massive β-cell apoptosis is observed (41). In this regard, C-peptide might be a possible regimen, along with insulin, for preventing end-stage diabetes complications.

In conclusion, high glucose can activate TG2 via sequential elevation of intracellular Ca^{2+} and ROS levels, which results endothelial cell apoptosis. C-peptide supplement therapy can prevent activation of transamidating activity and apoptosis in endothelial cells as well as in the aorta, heart, and kidney of diabetic mice. Thus, TG2 could be a potential therapeutic target for diabetes complications. These findings encourage further studies regarding the possibility of C-peptide supplement therapy together with insulin as a powerful approach for preventing diabetes complications in type 1 as well as in the late stage of type 2 DM.

ACKNOWLEDGMENTS

This work was supported in part by the Korea Research Foundation through the Basic Research Program (2008-05943) and the Ministry of Health and Welfare through the National R&D Program for Cancer Control (1020420).

No potential conflicts of interest relevant to this article were reported.

M.P.B. researched data and wrote the manuscript. Y.-C.L. researched data. J.H. and S.N. contributed to samples and discussion. Y.-M.K. contributed to discussion.

K.-S.H. is the guarantor of this work and, as such, had full access to all of the data in the study and takes responsibility for the integrity of the data and the accuracy of the data analysis.

REFERENCES

1. Massi-Benedetti M, Orsini-Federici M. Treatment of type 2 diabetes with combined therapy: what are the pros and cons? Diabetes Care 2008;31 (Suppl. 2):S131–S135
2. Wahren J, Ekberg K, Jörnvall H. C-peptide is a bioactive peptide. Diabetologia 2007;50:503–509
3. Geraldes P, Hiraoka-Yamamoto J, Matsumoto M, et al. Activation of PKC-delta and SHP-1 by hyperglycemia causes vascular cell apoptosis and diabetic retinopathy. Nat Med 2009;15:1298–1306
4. Isermann B, Vinnikov IA, Madhusudhan T, et al. Activated protein C protects against diabetic nephropathy by inhibiting endothelial and podocyte apoptosis. Nat Med 2007;13:1349–1358
5. Stoneman VE, Bennett MR. Role of apoptosis in atherosclerosis and its therapeutic implications. Clin Sci (Lond) 2004;107:343–354
6. World Health Organization. Global atlas on cardiovascular disease prevention and control [article online], 2011. Available from http://whqlibdoc.who.int/publications/2011/9789241564373 eng.pdf. Accessed 10 January 2012
7. Baumgartner-Parzer SM, Wagner L, Pettermann M, Gessl A, Waldhäusl W. Modulation by high glucose of adhesion molecule expression in cultured endothelial cells. Diabetologia 1995;38:1367–1370
8. Baumgartner-Parzer SM, Wagner L, Pettermann M, Grillari J, Gessl A, Waldhäusl W. High-glucose—triggered apoptosis in cultured endothelial cells. Diabetes 1995;44:1323–1327
9. Quagliaro L, Piconi L, Assaloni R, Martinelli L, Motz E, Ceriello A. Intermittent high glucose enhances apoptosis related to oxidative stress in human umbilical vein endothelial cells: the role of protein kinase C and NAD(P)H-oxidase activation. Diabetes 2003;52:2795–2804
10. Ho FM, Lin WW, Chen BC, et al. High glucose-induced apoptosis in human vascular endothelial cells is mediated through NF-kappaB and c-Jun NH2-terminal kinase pathway and prevented by PI3K/Akt/eNOS pathway. Cell Signal 2006;18:391–399
11. Inoguchi T, Li P, Umeda F, et al. High glucose level and free fatty acid stimulate reactive oxygen species production through protein kinase C–dependent activation of NAD(P)H oxidase in cultured vascular cells. Diabetes 2000;49:1939–1945
12. Dandona P, Thusu K, Cook S, et al. Oxidative damage to DNA in diabetes mellitus. Lancet 1996;347:444–445
13. Brownlee M. Biochemistry and molecular cell biology of diabetic complications. Nature 2001;414:813–820

14. Nishikawa T, Edelstein D, Du XL, et al. Normalizing mitochondrial superoxide production blocks three pathways of hyperglycaemic damage. Nature 2000;404:787–790
15. Brownlee M. The pathobiology of diabetic complications: a unifying mechanism. Diabetes 2005;54:1615–1625
16. Orrenius S, Zhivotovsky B, Nicotera P. Regulation of cell death: the calcium-apoptosis link. Nat Rev Mol Cell Biol 2003;4:552–565
17. Tamareille S, Mignen O, Capiod T, Rücker-Martin C, Feuvray D. High glucose-induced apoptosis through store-operated calcium entry and calcineurin in human umbilical vein endothelial cells. Cell Calcium 2006;39:47–55
18. Park D, Choi SS, Ha KS. Transglutaminase 2: a multi-functional protein in multiple subcellular compartments. Amino Acids 2010;39:619–631
19. Yoo JO, Lim YC, Kim YM, Ha KS. Differential cytotoxic responses to low- and high-dose photodynamic therapy in human gastric and bladder cancer cells. J Cell Biochem 2011;112:3061–3071
20. Ou H, Haendeler J, Aebly MR, et al. Retinoic acid-induced tissue transglutaminase and apoptosis in vascular smooth muscle cells. Circ Res 2000;87:881–887
21. Kuo TF, Tatsukawa H, Matsuura T, Nagatsuma K, Hirose S, Kojima S. Free fatty acids induce transglutaminase 2-dependent apoptosis in hepatocytes via ER stress-stimulated PERK pathways. J Cell Physiol 2012;227:1130–1137
22. Nadalutti C, Viiri KM, Kaukinen K, Mäki M, Lindfors K. Extracellular transglutaminase 2 has a role in cell adhesion, whereas intracellular transglutaminase 2 is involved in regulation of endothelial cell proliferation and apoptosis. Cell Prolif 2011;44:49–58
23. Song H, Kim BK, Chang W, et al. Tissue transglutaminase 2 promotes apoptosis of rat neonatal cardiomyocytes under oxidative stress. J Recept Signal Transduct Res 2011;31:66–74
24. Hills CE, Brunskill NJ. Cellular and physiological effects of C-peptide. Clin Sci (Lond) 2009;116:565–574
25. Hills CE, Brunskill NJ, Squires PE. C-peptide as a therapeutic tool in diabetic nephropathy. Am J Nephrol 2010;31:389–397
26. Ido Y, Vindigni A, Chang K, et al. Prevention of vascular and neural dysfunction in diabetic rats by C-peptide. Science 1997;277:563–566
27. Chima RS, LaMontagne T, Piraino G, Hake PW, Denenberg A, Zingarelli B. C-peptide, a novel inhibitor of lung inflammation following hemorrhagic shock. Am J Physiol Lung Cell Mol Physiol 2011;300:L730–L739
28. Mughal RS, Scragg JL, Lister P, et al. Cellular mechanisms by which proinsulin C-peptide prevents insulin-induced neointima formation in human saphenous vein. Diabetologia 2010;53:1761–1771
29. Cifarelli V, Luppi P, Tse HM, He J, Piganelli J, Trucco M. Human proinsulin C-peptide reduces high glucose-induced proliferation and NF-kappaB activation in vascular smooth muscle cells. Atherosclerosis 2008;201:248–257
30. Kobayashi Y, Naruse K, Hamada Y, et al. Human proinsulin C-peptide prevents proliferation of rat aortic smooth muscle cells cultured in high-glucose conditions. Diabetologia 2005;48:2396–2401
31. Li ZG, Zhang W, Sima AA. C-peptide enhances insulin-mediated cell growth and protection against high glucose-induced apoptosis in SH-SY5Y cells. Diabetes Metab Res Rev 2003;19:375–385
32. Sima AA, Li ZG. The effect of C-peptide on cognitive dysfunction and hippocampal apoptosis in type 1 diabetic rats. Diabetes 2005;54:1497–1505
33. Cifarelli V, Geng X, Styche A, Lakomy R, Trucco M, Luppi P. C-peptide reduces high-glucose-induced apoptosis of endothelial cells and decreases NAD(P)H-oxidase reactive oxygen species generation in human aortic endothelial cells. Diabetologia 2011;54:2702–2712
34. Yi SJ, Kim KH, Choi HJ, et al. [Ca(2+)]-dependent generation of intracellular reactive oxygen species mediates maitotoxin-induced cellular responses in human umbilical vein endothelial cells. Mol Cells 2006;21:121–128
35. Park JY, Jung SH, Jung JW, et al. A novel array-based assay of in situ tissue transglutaminase activity in human umbilical vein endothelial cells. Anal Biochem 2009;394:217–222
36. Gallo A, Ceolotto G, Pinton P, et al. Metformin prevents glucose-induced protein kinase C-beta2 activation in human umbilical vein endothelial cells through an antioxidant mechanism. Diabetes 2005;54:1123–1131
37. Rigler R, Pramanik A, Jonasson P, et al. Specific binding of proinsulin C-peptide to human cell membranes. Proc Natl Acad Sci USA 1999;96:13318–13323
38. Luppi P, Geng X, Cifarelli V, Drain P, Trucco M. C-peptide is internalised in human endothelial and vascular smooth muscle cells via early endosomes. Diabetologia 2009;52:2218–2228
39. Li ZG, Qiang X, Sima AA, Grunberger G. C-peptide attenuates protein tyrosine phosphatase activity and enhances glycogen synthesis in L6 myoblasts. Biochem Biophys Res Commun 2001;280:615–619
40. Jägerbrink T, Lindahl E, Shafqat J, Jörnvall H. Proinsulin C-peptide interaction with protein tyrosine phosphatase 1B demonstrated with a labeling reaction. Biochem Biophys Res Commun 2009;387:31–35
41. Prentki M, Nolan CJ. Islet beta cell failure in type 2 diabetes. J Clin Invest 2006;116:1802–1812